EVALUATION OF THE SEISMIC VULNERABILITY OF THE "ANCIEN HÔPITAL DE SION" USING APPLIED ELEMENT MODELLING (AEM) AND LOCAL MECHANISM ANALYSIS

Angelo Garofano and Pierino Lestuzzi

École Polytechnique Fédérale de Lausanne (EPFL), EPFL ENAC IIC IMAC, Lausanne, Switzerland

Abstract:

The evaluation of the seismic vulnerability of monumental buildings is a difficult task and presents significantly higher level of complexity if compared to the case of new or current existing structures. This is due to the inherent uncertainty characterizing ancient buildings, regarding structural characteristics and constructive techniques, material properties, damages due to past actions, which should be properly handled in their seismic assessment. For this reason, the approach to the study of such buildings unavoidably involves the completion of different assessment methods and their comparison, in order to represent the characteristics of a complex structure, its local and global behaviour. This paper describes the first results of the evaluation of the seismic safety of the "Ancien Hôpital de Sion", an important building belonging to the Swiss architectural heritage, sited in the Canton of Valais, the region with the highest seismic hazard in Switzerland. For the analysis of the building, three-dimensional Applied Element (AEM) modelling of the whole structure has been achieved and validated. The proposed modelling strategy, together with non-linear dynamic analysis, has been adopted on the basis of its capability to represent the actual behaviour and failure mechanisms of complex masonry structures, in addition to a good computational efficiency compared to other available numerical approaches. The local seismic collapse mechanisms have been also analysed through a kinematic limit analysis based on rigid block rotation. Both linear and non-linear approaches have been followed together with the capacity spectrum method. The results provided by the different methodologies have been compared with the aim to provide possible insights concerning a general procedure for the assessment of the safety of such type of structures.

Keywords: Seismic Behaviour, Historical Constructions, Applied Element Method (AEM), Non-linear Dynamic Analysis, Macro-element Analysis.

1 INTRODUCTION

The study of historical constructions presents many challenging aspects and often requires the application of different analysis methods and modelling techniques in order to satisfactorily describe their actual behaviour. A comprehensive and multidisciplinary procedure should be followed when approaching the assessment of the seismic vulnerability of heritage masonry buildings with the possibility to adapt different techniques to their particular charachteristics [1]. It is necessary, therefore, to combine both traditional and innovative investigation techniques with different level of complexity and detail of analysis. Simplified methods must be representative of particular aspects of the structural behaviour, yet support and validate the reliability of the results provided by more refined analysis procedures [2].

The present paper focuses on the study of a historical masonry building, the *Ancien Hôpital de Sion*, belonging to the Swiss architectural heritage and listed in the ISOS inventory (Federal Inventory of Swiss Heritage Sites). The building is located in the Canton of Valais, the region with the highest seismic hazard in Switzerland, therefore the assessment of its seismic vulnerability represents a crucial aspect within the phases of protection and safeguard of this important structure. The building represents a complex masonry structure, therefore different assessment methods have been considered for its study.

A three-dimensional Applied Element (AEM) model of the whole structure has been developed for non-linear dynamic analyses. Compared to the Finite Element Method (FEM), in the AEM the structure is discretized through an assemblage of relatively small elements connected by a set of non-linear springs located at contact points distributed along the element faces. Normal and shear springs transfer the normal and shear stresses between the elements. Through the springs it is possible to represent the non-linear material behaviour, the element separation or contact, and eventual collision [3, 4].

The possibilities of the AEM to overcome the drawbacks of FEM have been explored in the present work in the case of a masonry building subjected to a seismic excitation. The adopted modelling strategy has been employed to simulate the actual behaviour of the building and the possible failure mechanisms of a complex masonry structure.

In addition, the possible local collapse mechanisms of the building have been studied by means of a kinematic limit analysis, based on the decomposition into rigid macro-elements which can be individuated after the observation of typical seismic failure modes of existing masonry structures [5]. This is a useful method particularly for the study of buildings which do not feature a box behaviour under seismic actions due to the lack of stiff floors or weakening of connections between walls due to pre-existing damages. In the present case, both linear and non-linear static approaches have been followed in combination with the capacity spectrum method [6, 7].

2 DESCRIPTION OF THE BUILDING

The construction of the *Ancien Hôpital de Sion* took place between 1763 and 1781 (Figure 1a) and it served as a hospital until 1937 [8, 9]. Presently, the Ancien Hôpital constitutes a representative and distinctive building of the city of Sion and it is placed under the protection of the Swiss Confederation. Due to its important role within the city and for its architectural quality, the building is listed in the ISOS inventory (Federal Inventory of Swiss Heritage Sites).

The building is an isolated structure, without any connection with surrounding buildings, as it can be seen from the general view in Figure 2a. A view of the building's main façade is shown in Figure 2b.

The Ancien Hôpital is a masonry building with timber slabs composed by a central body and two external wings (the Aile Nord and the Aile Sud) connected at its extreme sides forming a C-shaped floor plan (see Figure 1b). The building has three storeys over the ground floor, with a basement level under the central and southern areas of the structure. The overall in-plane dimensions of the building are 50 m x 42 m. The height of the ground and first level is 3.60 m, while the height of the second level is 3.30 m.

The structure's roof is a timber truss assembly [10, 11], reaching a total height of 17 m. The central part of the main body of the Ancien Hôpital is occupied by a chapel with a vaulted timber structure, surmounted by a tower with a total height of 26 m. The thickness of the masonry walls varies from about 1 m at the lower level to about 0.8 m at the higher levels.
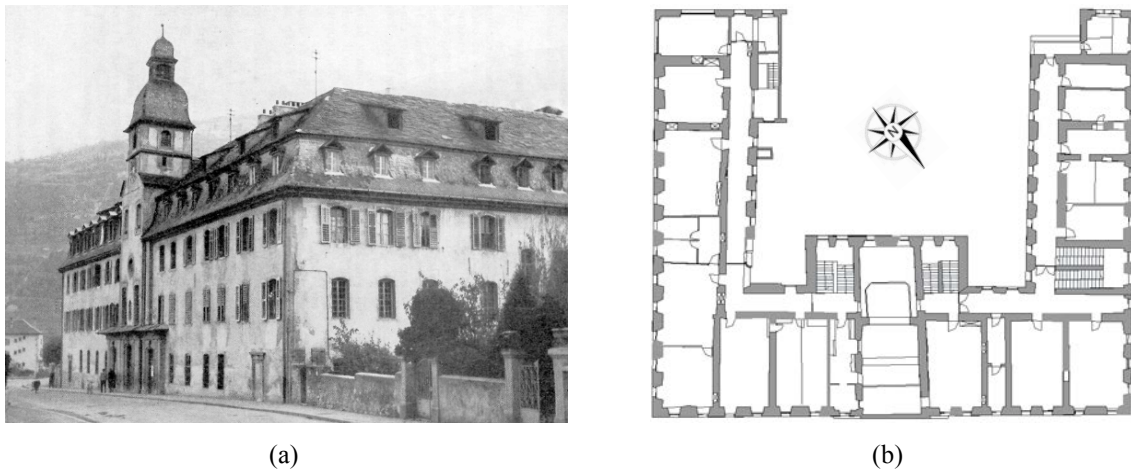

(a)   (b)

Figure 1: Historical image of the Ancien Hôpital [8] (a) and ground level floor plan [10] (b).

(a)   (b)

Figure 2: Top view of the building in the historical center of the city of Sion (a) and view of the building's façade (b) *(Source: Map data ©2015 Google).*

On the occasion of some restoration works completed in 2012 on the Northern wing, visual inspection and hole drilling were performed with the aim to define the masonry typology. The original stones used for the masonry are irregularly shaped, but they are optimally arranged and the overall conservation status of mortar joints was good (see Figure 3a).

The slabs found in the structure are made with timber beams having approximatively squared cross-section, with a timber layer, a mortar layer and the pavement. An example is

3

shown in Figure 3b. The slabs have been subjected to a survey and non-destructive testing for characterization of materials and for the evaluation of their bearing capacity in 2012 [12, 13]. Three classes were identified through ultrasonic in-situ testing, C18, C24 and C30, according to the European Norm EN338 [14]. In general, the beams were mainly belonging to the class of strength C30, while some C24 class beams were also found in the Southern wing and few C18 class in the Northern wing. The surveyed beams presented squared cross-sections of about 20 cm x 20 cm, with interspacing of 45-50 cm and supported length of about 30 cm.
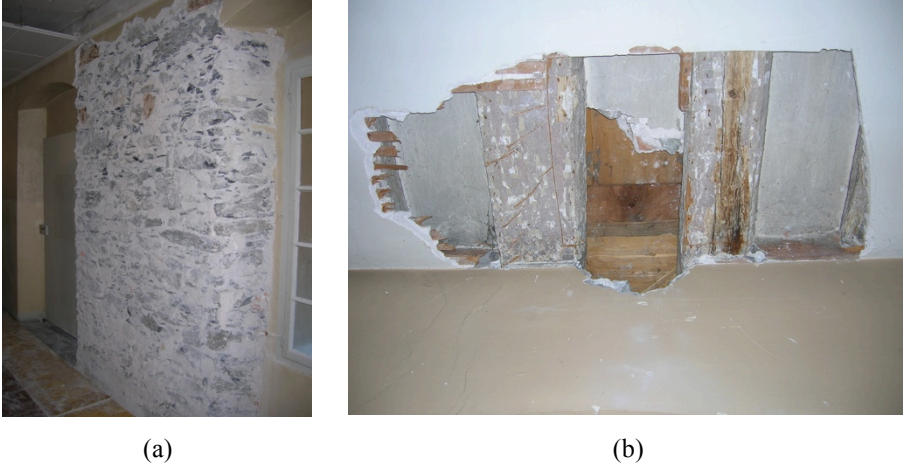

(a)   (b)

Figure 3: Example of masonry (a) and bottom view of a slab typology (b) found in the structure [12].

3   SEISMIC HAZARD AT THE BUILDING SITE

The city of Sion is provided with a microzonation study for the distribution of the seismic hazard over the territory, identifying three seismic zones [15]. The Ancien Hôpital lies along the dividing line between two different zones; therefore, given the importance of the structure, a specific evaluation of the response spectrum was carried at the building site (dashed line in Figure 4b).
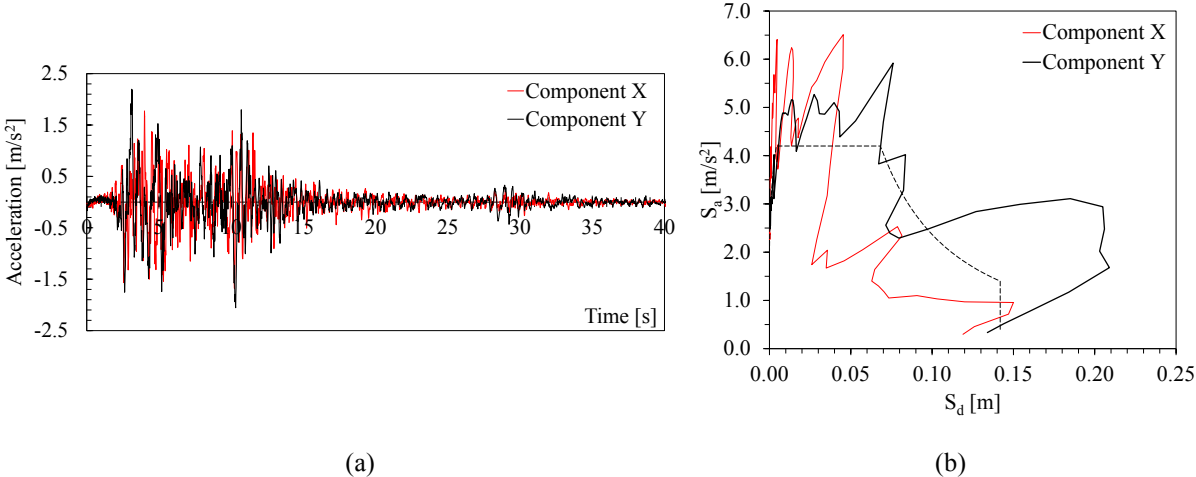

(a)   (b)

Figure 4: Record ESD 198 (European Strong Motion Database, Montenegro Earthquake, M_S = 7.1, PGA = 0.224g): recorded ground accelerations in X and Y directions (a) and elastic response spectra (ADRS format) of the corresponding earthquake components for 5% damping (b).

In order to perform time-history dynamic analyses of the building, some records of seismic events respectful of the best fitting with the response spectrum provided for the Ancien

Hôpital were selected from international databases. One of these was represented by the Component Y of the Record ESD 198, with associated PGA = 0.224g. In particular, the model was subjected to the seismic registration reported in Figure 4a, illustrating the X (N-S) and Y (E-W) components of the recorded ground accelerations. The corresponding elastic response spectra for 5% damping are illustrated in Figure 4b, together with the response spectrum (dashed line) proposed for the site of the Ancien Hôpital for a comparison.

4 NUMERICAL MODELLING

4.1 Adopted modelling strategy

The methodology followed for the numerical modelling of the studied building is based on the Applied Element Method (AEM). This method represents an alternative modelling technique to the Finite Element Method and has been used in combination with non-linear dynamic analysis [4, 16, 17].

Considering the mechanical behaviour of a masonry building and the interaction between the structural elements, the Applied Element Method (AEM) gives the advantage to allow to consider all the possible failure mechanisms. The AEM method is based on dividing the masonry elements in small elements connected through springs (see Figure 5a). According to this strategy, there are no common nodes between elements and, therefore, it is possible to easily describe large displacements and elements progressive separation through successive failure of these springs [3]. Normal and shear springs located at the element contact points, distributed around the edges, as shown in Figure 5b, represent stresses, strains, and deformations of certain portions of the structure. Figure 5c illustrates an example of the configuration of springs between two elements, extended from the centreline of one element to the centreline of the adjacent one.

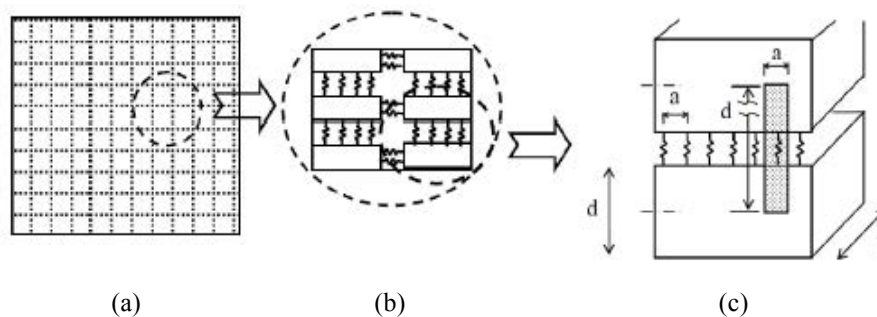
| (a) | (b) | (c) |

Figure 5: Masonry element modelling with AEM: element generation (a); spring distribution (b); area of influence of each springs pair (c) (Adapted from [16]).

For the studied masonry building, a total number of five springs was used on each face of the elements. The size of the meshing was selected and opportunely validated to avoid creating elements with large aspect ratios. In Figure 6 different views of the AEM model of the building are reported. The timber slabs have been modelled too according to the actual disposition in the structure.

Two models have been prepared, considering two different element sizes for masonry walls: a refined mesh (element dimensions ≤ 0.4 m) with two elements in the wall thickness and a large mesh division (element dimensions ≤ 0.8 m), with only one element in the wall thickness. This two cases were analysed with respect to the accuracy of the provided results and computational time requirements.
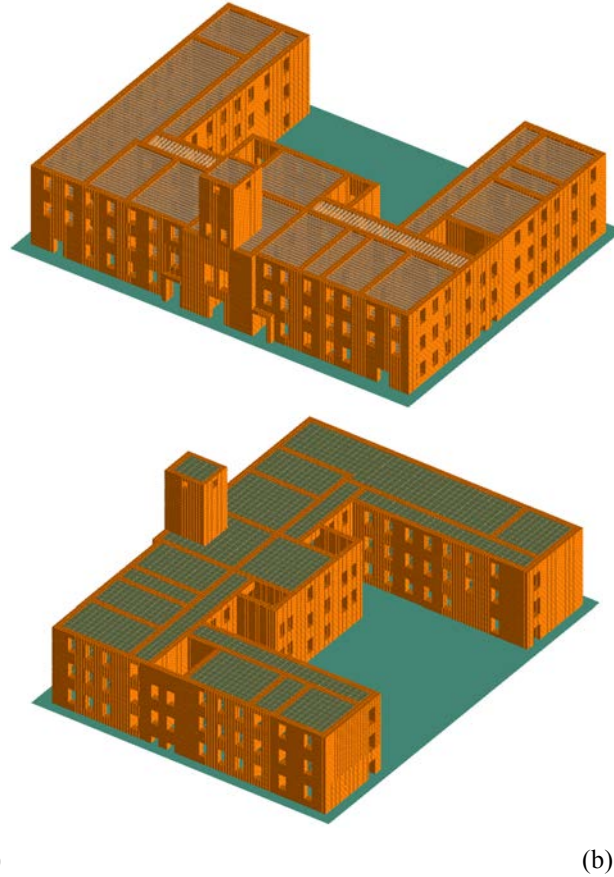
5

| (a) | (b) |

Figure 6: Three-dimensional numerical model of the building with view of timber beams and slab (Refined mesh).

4.2 Failure criterion for masonry

Specific material models are assigned to the springs connecting the different applied elements in the AEM. Therefore, different material properties are described through the springs' characteristics, which are used to calculate strains, stresses and failure criteria [18]. Masonry is modelled similarly to concrete, adopting the Maekawa compression model including unloading and reloading [19], shown in Figure 7a. In this model, the envelope of compressive stress-strain diagram is defined using three values: the initial Young's modulus, the fracture parameter, representing the extent of the internal damage, and the compressive plastic strain. For the tensile behaviour, the relationship is linear until the cracking point. After cracking, stiffness of springs subjected to tension is set to zero. The residual stresses are then redistributed in the next loading step by applying the redistributed force values in the reverse direction. The material is assumed to crack when the major principal stress reaches the tensile strength.

Regarding the shear behaviour, the tangent modulus is calculated according to the strain at the spring location. After peak stresses, spring stiffness is assumed as a minimum value to avoid negative stiffness. This results in a difference between the calculated the stress and stress corresponding to the spring strain. These residual stresses are redistributed by applying the redistributed force values in the reverse direction in the next loading step. The relationship between shear stress and shear strain is assumed to remain linear till the cracking. Then, the shear stresses drop down as shown in Figure 7b. The level of drop of shear stresses depends on the aggregate interlock and friction at the crack surface.
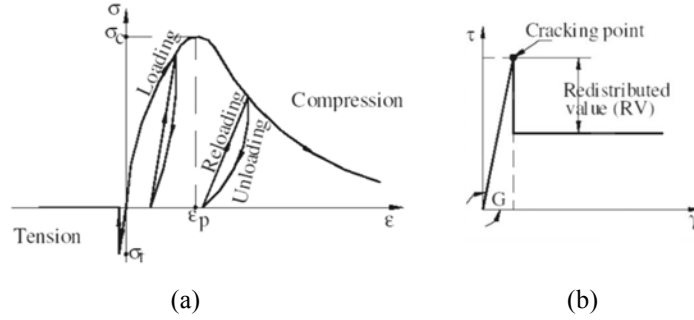
6

Figure 7: Constitutive models adopted for masonry under axial (a) and shear (b) stresses.

When the separation strain is reached, the adjacent elements are totally separated at the connecting face. In this case, all the springs are cut and, if the elements meet again during the analysis, they behave as two different rigid bodies in contact. When contact occurs between elements, linear springs are generated at contact points, governed by parameters such as the normal and shear contact stiffness factors and the contact spring unloading stiffness factor. During new contact friction between masonry portions is possible and depends on the friction coefficient value. There is no internal friction inside structural components which are already connected by normal and shear springs, and the friction coefficient has effect only after element separation when elements meet as rigid bodies. Mechanical parameters assumed in the analysis are reported in Table 1.

Unit weight [kN/m^3]	21
Young's modulus [N/mm^2]	1500
Shear modulus [N/mm^2]	700
Tensile strength [N/mm^2]	0.25
Compressive strength [N/mm^2]	3
Separation strain [−]	0.1
Friction coefficient [−]	0.8
External damping ratio [−]	0
Normal contact stiffness factor [−]	$1 \cdot 10^{-4}$
Shear contact stiffness factor [−]	$1 \cdot 10^{-5}$
Contact spring unloading stiffness factor [−]	2

Table 1: Mechanical parameters for masonry.

4.3 Modal analysis

From the analysis of the modal shapes of the building, the first two modes involve the vibration in the two principal directions of the central tower (see Figure 8a and 8b), which is also expected to be the most vulnerable part of the structure. The following modes involve mainly one or both lateral wings of the building. The vibration modes are the same in the case of the refined and large mesh division.

For both mesh divisions, the values of the periods for the first six modes are reported in Table 2. The differences in the periods when considering the refined mesh instead of the large mesh are negligible (lower than 3% for the first three modes), thus confirming the reliability of the model with large mesh from the dynamical point of view.

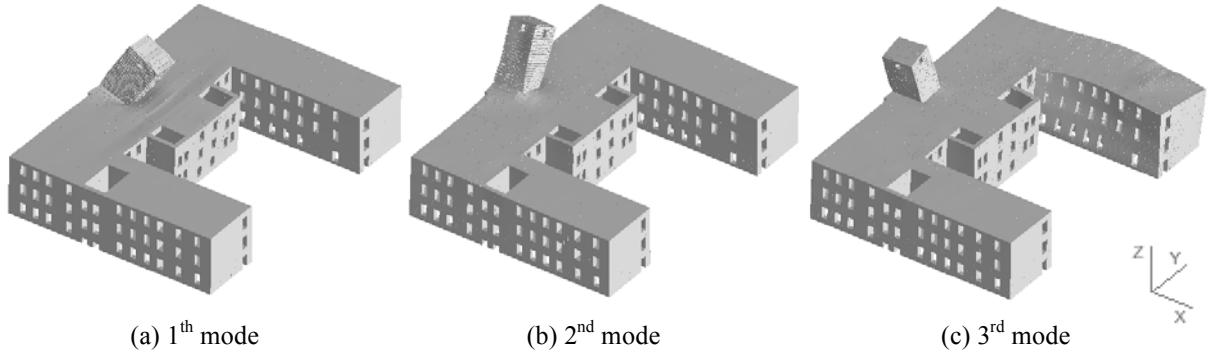| (a) 1th mode | (b) 2nd mode | (c) 3rd mode |

Figure 8: Modal shapes of the building.

For the first three modes, the variation of the values of the periods is reported in Figure 9 in order to have an indication on the damage progression during the acceleration time-history. In particular, the irregular path in the variation of the first mode's period reveals the damage of the tower with out-of-plane collapse in the X direction. The comparison of the two mesh divisions showed, in this case, the tendency of the values of periods associated to the refined mesh to reduce more than in the case of the normal mesh for higher time steps of the analysis. Therefore, a higher susceptibility of the model with refined mesh to present higher damage was found.

During the study of the building, the modal shapes have been also compared to the case of the structure without the timber slabs in order to simulate an extreme case of completely ineffective connection at the floor level between the masonry walls. As expected, in this case the modal shapes involved firstly single walls of the structure before the central tower.

Mode	Refined mesh T [s]	Large mesh T [s]	Δ [%]
1	0.222	0.219	+1.4
2	0.215	0.218	+1.5
3	0.175	0.170	+2.7
4	0.155	0.151	+2.6
5	0.143	0.140	+2.7
6	0.131	0.126	+3.4

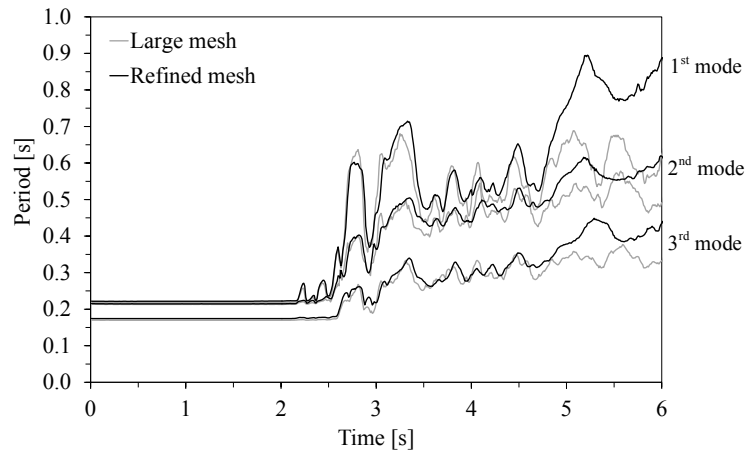Table 2: Periods and frequencies.

Figure 9: Period variation for the first three modes and comparison between large and refined mesh.

8

4.4 Time-history dynamic analysis

The dynamic analysis carried out considering the recorded time-history reported in Figure 4 allowed to confirm that the most vulnerable part of the structure is the central tower, which presented out-of-plane damages. However, the rest of the building did not suffer high damage due to the application of this seismic registration. The most evident crack is located in the middle of the back wall of the Southern wing.

In a second phase, time-history analysis have been repeated in order to evaluate the level of ground acceleration responsible of damage in the structure of the hospital. The record considered in the previous case was therefore amplified through the application of a factor of 2 to the acceleration ordinates. In this case the seismic action is characterized by a double value of PGA and the corresponding spectrum can be representative of seismic demand with a higher return period.

The resulting damage distribution can be seen from Figure 10, where it can be noted that the considered ground acceleration record was responsible of the opening of several cracks. In particular, higher damage is located at the back corner of the Southern wing, where the connection of between the two converging walls is lost (see also Figure 12a and 12b). Severe damage was also obtained at the back of the central body of the building, involving the walls enclosing the staircases. In these areas, cracks opened at the intersection of the corner walls with the central body of the building, initiating the overturning of the whole corner or possibly of the single walls separately (see Figure 10 and 12a). The Northern wing of the building suffered more distributed damage, with cracks mainly located in the piers and starting from the openings. Again, the masonry walls in the area of the staircase suffered higher damage (see Figure 12c).
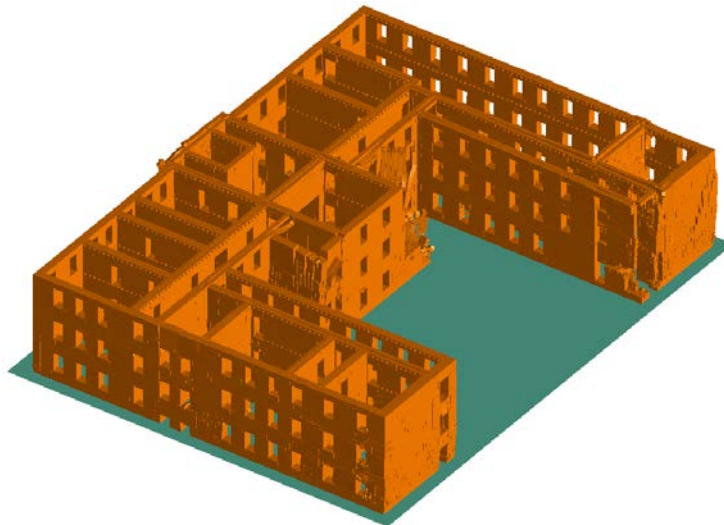

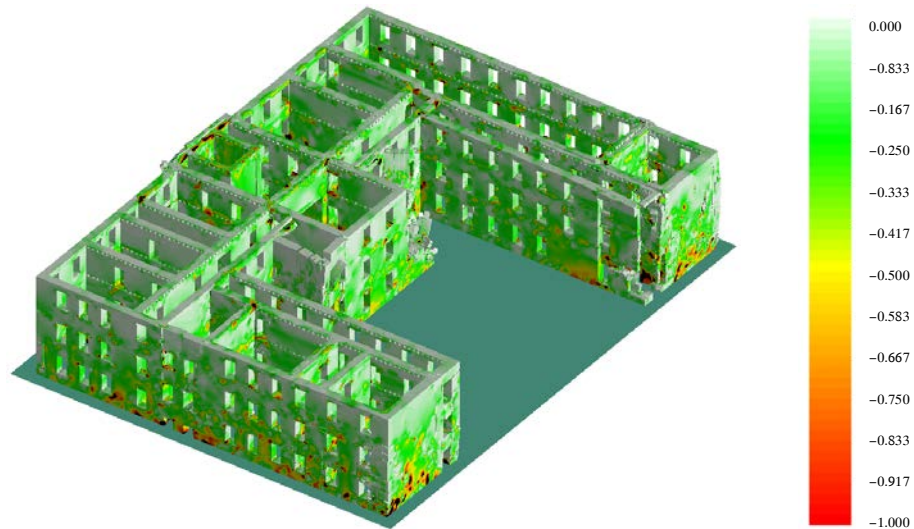Figure 10: Damage distribution (X20) at the last time step (t = 40 s).

Figure 11: Compressive principal stress distribution (N/mm^2) at last time step (t = 40 s).

In Figure 11, the principal compressive stress distribution is illustrated over the damaged structure at the last time step of the analysis. The areas in dark red are characterized by a compressive stress higher than 1 N/mm^2 (it is reminded that the compressive strength of the masonry is 3 N/mm^2). The compressive damage involves only quite limited portions of masonry mainly localized at the lower zones of the ground level's masonry walls.

In Figure 12, the damage distribution obtained from the model with large mesh division and the model with refined mesh division is reported for the same walls of the building. From the comparison, it can be noted that the refined model is able to provide a more precise cracking distribution and a higher damage level (full overturning of some portions of masonry). However, the computational cost associated to the model with large mesh division is sensibly lower and represent an advantage in terms of time saving.
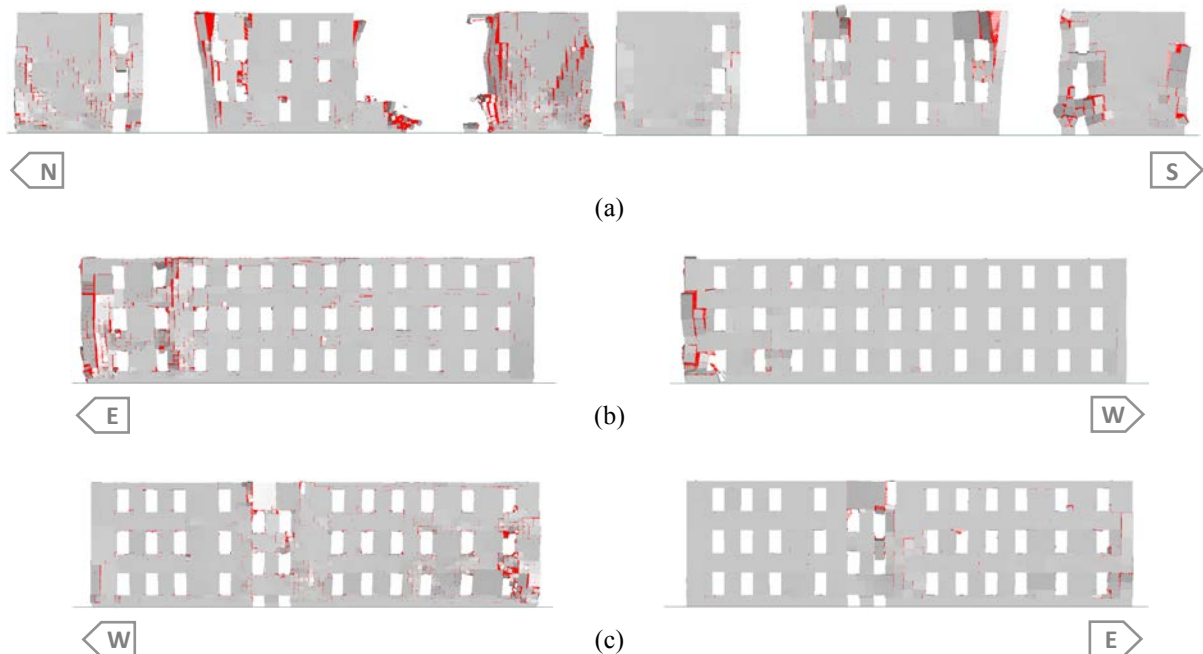

Figure 12: Damage distribution (X20) and cracking pattern at last time step (t = 40 s) for: (a) Eastern walls; (b) Southern walls; (c) Northern walls. (Elements dimensions ≤ 0.4 m (left) and ≤ 0.8 m (right)).

10

The influence of the horizontal elements plays a fundamental role in the response of an existing masonry building to the seismic action. However, the correct modelling of the slabs and representation of the actual connection conditions with the vertical masonry elements is a questionable point and sometimes can be carried out only thought very refined and time consuming models.

In order to compare the behaviour of the building in the case of very poor connection between the timber slabs and the masonry walls, a model without slabs was also employed in the analyses, representing an extreme condition for the stiffness of the horizontal elements and for the connection between the vertical elements.

The analysis was carried out considering the ground acceleration record amplified by 2, obtaining the damage distribution illustrated in Figure 13. The comparison of the damage distribution (Figure 10) with the one obtained in the case with slabs showed the higher damage suffered by the structure and a higher number of involved walls in the case without slabs, evidencing the important role of the slab stiffness in the seismic response of the structure.
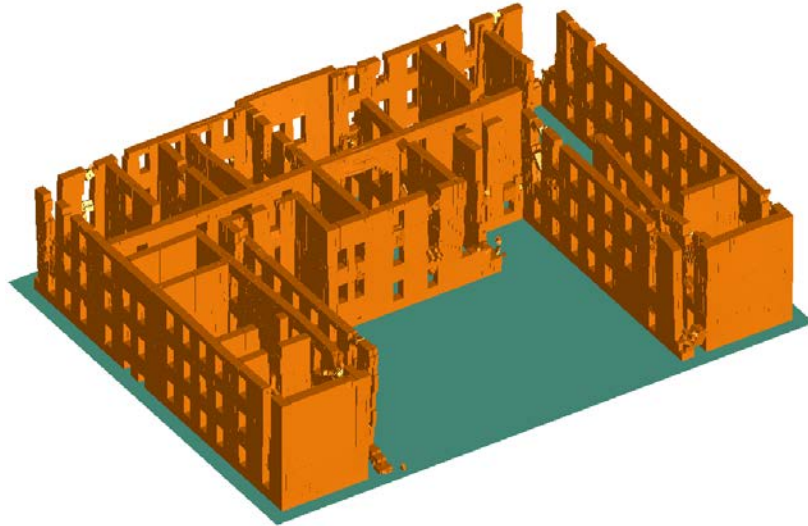

Figure 13: Damage distribution in the model without slabs at the last time step (t = 40 s).

5   ANALYSIS OF THE LOCAL COLLAPSE MECHANISMS

The safety of the structure was assessed through the analysis of different possible local collapse mechanisms following the linear and non-linear approaches [5, 20, 21]. The zones of the structure considered more likely vulnerable to overturning effects were identified for the calculations.

The kinematic linear approach allows to define the value of the load multiplier, α_0, connected to the horizontal force that the element is able to withstand. In terms of acceleration, the safety of the structure against the considered collapse mechanism is satisfied if:

$$a^*_0 \geq a_{g(SLU)} \tag{1}$$

where $a_{g(SLU)}$ is the acceleration demand imposed by the earthquake calculated assuming a strength reduction factor equal to 2 [22].

Following the non-linear approach, the safety of the structure is carried out through the comparison between the ultimate displacement capacity, represented by d^*_u (assumed as 40% of the spectral displacement, d^*_0, corresponding to a null value of a^* [22]), and the displacement demand, $\Delta_d = S_{De}(T_s)$, obtained from the displacement spectrum for the secant period, T_s:

$$d^*_u \geq \Delta_d \tag{2}$$

As an example, the analysis of the mechanisms involving the Southern façade of the building is shown in Figure 14, considering an importance factor, $\gamma_I = 1.2$. The comparison between seismic demand and capacity is graphically reported in ADSR format.

The results of the analysis for some of the mechanisms are summarized in Table 3, reporting the safety coefficients, α_{eff}, obtained both from the linear and the non-linear kinematic approaches and for importance factors, γ_I, equal to 1.2 and 1.
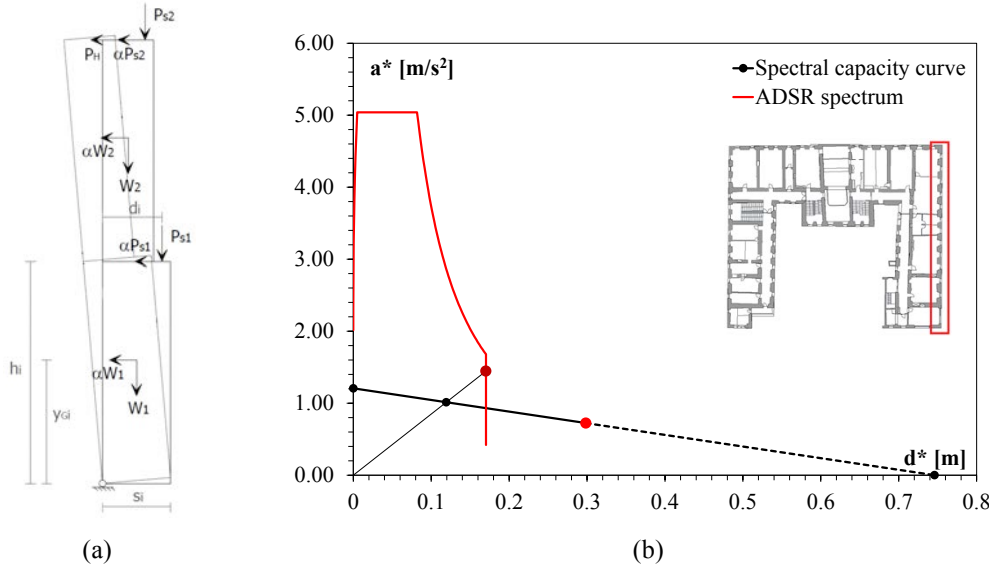

(a)   (b)

Figure 14: Example of overturning mechanism for masonry wall (two levels) (a) and spectral capacity curve and safety verification of the overturning of the Southern façade (b).

Mechanism	Importance factor $\gamma_I = 1.2$		Importance factor $\gamma_I = 1$	
	α_{eff} [−]		α_{eff} [−]	
	Linear analysis	Non-linear analysis	Linear analysis	Non-linear analysis
Southern façade	1.20	1.75	1.44	2.10
South-Eastern corner	1.72	2.97	2.06	3.56
Central staircase corner	2.23	3.26	2.68	3.92
Central staircase wall	0.75	0.94	0.90	1.13

Table 3: Summary of safety factors from the analysis of local mechanisms.

6 CONCLUSIONS AND FUTURE DEVELOPMENTS

The *Ancien Hôpital de Sion* is an important heritage structure located in the Canton of Valais, the region with the highest seismic hazard in Switzerland. The present paper aimed at the assessment of the seismic safety of such historical building through different approaches.

For the numerical modelling of the structure, the Applied Element Method (AEM) was followed and allowed to account for all possible failure modes of masonry.

The non-linear dynamic analysis carried out with an acceleration time history compatible with the site response spectrum evidenced that the building is able to stand the seismic action expected at the site suffering minor damaging.

When the acceleration is amplified by a factor of two (higher return period), the structure suffered cracking of several masonry walls, loss of connection at some corners and overturning of portions of masonry. The damage was more significant in the area of the Southern wing and in the walls enclosing the staircases. Higher cracks concentration at the connecting areas of the lateral wings with the central body was observed.

The building features a masonry tower in the central part of the main body, where a vaulted chapel is also located. This constitutes the most vulnerable element of the building and it is characterized by high damage even when the lower seismic action was considered. The structure and the behaviour of the central tower require deeper investigation and characterization in terms of construction technique and materials and to be studied with more detailed analyses.

Another point of interest evidenced by the numerical analysis concerns the level of connection between the slabs, through the timber beams, and the bearing masonry walls. The comparison between the model including the timber slabs according to the actual geometry and direction of beams, and a model with free walls showed the importance of the presence of the slabs in case the structure is subjected to a seismic action.

The study of possible local collapse mechanisms allowed to identify the most vulnerable parts of the structure. The safety factors are higher than one except for the case of the central staircase wall at the back of the building. The safety coefficients associated to a single wall are 0.9 from the linear approach and 1.13 from the non-linear approach, indicating the possible overturning of the wall for an action slightly higher than 1 (non-amplified registration). In comparison, the model subjected to the non-amplified seismic registration, showed a diffuse cracking in the area of this wall, but without reaching its out-of-plane failure. Therefore, in this case the application of the mechanisms analysis is more conservative, particularly in the linear approach.

Safety factors higher than 2 are obtained for the central staircase corner. In fact, the model subjected to an acceleration amplified by two showed that vertical cracks form at this corner with subsequent overturning of the two converging walls separetely, instead of the whole corner. For the Southern façade and the South-Eastern corner, the results of the numerical analysis are intermediate between the results given by the linear and the non-linear approaches. The model showed severe cracking and disconnection of masonry at the corners, but without complete overturning of the walls. Therefore, also in this case the application of the linear approach resulted to be more conservative than the non-linear approach which was found more realistic.

REFERENCES

[1] F. Ceroni, M. Pecce, S. Sica, A. Garofano, Assessment of seismic vulnerability of a historical masonry building. *Buildings, MDPI, Special Issue: Earthquake Resistant Buildings*, 2012; 2(3):332-358. DOI: 10.3390/buildings2030332.

[2] F. Ceroni, A. Garofano, M. Pecce, Seismic behaviour of masonry buildings: application of different approaches to a case study. *14th European Conference of Earthquake Engineering*, 30.08-03.09.2010 Ohrid, Macedonia, CD Rom.

[3] K. Meguro, H.R. Tagel-Din, Applied element simulation of RC structures under cyclic loading. *Journal of Structural Engineering*, Vol. 127, No. 11, November, 2001.

[4] H.R. Tagel-Din, K. Meguro, Analysis of a small scale RC building subjected to shaking table tests using applied element method. *Proceedings of the 12th World Conference on Earthquake Engineering,* New Zealand, pp. 25–34, January 30 – February, 2000.

[5] C.F. Carocci, Guidelines for the safety and preservation of historical centres in seismic areas. In: *Historical constructions*. University of Minho, Guimaraes, pp 145–165, 2001.

[6] P. Fajfar, Capacity spectrum method based on inelastic demand spectra. *Earthquake Engineering and Structural Dynamics*, 28:979–993, 1999.

[7] S. Lagomarsino, On the vulnerability assessment of monumental buildings. *Bulletin of Earthquake Engineering*, 4:445–463. European Comission, Brussels, 2006.

[8] S. Crettaz, Hôpital de Sion (XIIe au XXe siècle). In: *Annales Valaisannes, Société d'Histoire du Valais Romand*, 1949, 145-180, fig. (dont 1 portr.). (In French).

[9] P. de Rivaz, Les hôpitaux de Sion. In: *Annales Valaisannes, Société d'Histoire du Valais Romand*, 1940, 44-48. (In French).

[10] CERT Ingénierie SA, *Ville de Sion. Rénovation de l'Ancien Hôpital. Étude de faisabilité: toiture, plancher et colombage.* 20 Novembre 2009. (In French).

[11] Lignum-Cedotec, *Rapport "Ancien Hôpital de Sion" - Charpente et planchers en bois*. 2 June 2009. (In French).

[12] CERT Ingénierie SA, *Ville de Sion. Rénovation de l'Ancien Hôpital. Rapport d'évaluation de la capacité portante des planchers en bois.* Rapport AVP101, 5 June 2012. (In French).

[13] Concept Bois Technologie, *Evaluation de la résistance résiduelle de poutres en bois constituant le plancher de l'Ancien Hôpital de Sion (VS). Mesures sur échantillonnage.* Rapport d'expertise, 12 May 2012. (In French).

[14] European Commitee for Standardization (CEN), *EN 338 - Structural timber. Strength classes*. 2009.

[15] Centre de recherche sur l'environnement alpin (CREALP): www.crealp.ch

[16] A. Karbassi, P. Lestuzzi, Fragility analysis of existing unreinforced masonry buildings through a numerical-based methodology. *The Open Civil Engineering Journal*, vol. 6, (Suppl 1-M2) 121-130, 2012.

[17] A. Karbassi, M.-J. Nollet, Performance based seismic vulnerability evaluation of masonry buildings using Applied Element Method in a nonlinear dynamic-based analytical procedure. *Earthquake Spectra*, Vol. 29, No. 2, 399-426, 2013.

[18] Applied Science International. *Extreme Loading® for Structures (Version 3.1), Theoretical Manual; Modelling Manual*, Durham, NC, 2013.

[19] H. Okamura, K. Maekawa, *Nonlinear analysis constitutive models of reinforced concrete*. Gihodo Co. Ltd., Tokyo, 1991.

[20] F. Papa, G. Zuccaro, Un modello di valutazione dell'agibilità post-sismica attraverso la stima dei meccanismi di collasso. *XI Congresso Nazionale ANIDIS "L'Ingegneria Sismica in Italia",* Genova, 2004.

[21] M.C. Griffith, G. Magenes, G. Melis, L. Picchi, Evaluation of out-of-plane stability of unreinforced masonry walls subjected to seismic excitation. *Journal of Earthquake Engineering*, Vol. 7, Special Issue 1, 141-169, 2003.

[22] Circolare 617. *Istruzioni per l'applicazione delle "Nuove norme tecniche per le costruzioni di cui al D.M. 14 gennaio 2008.* Ministero dei Lavori Pubblici, Roma, 02/02/2009. (In Italian).